

## Article

# A Novel Method for Traffic Estimation and Air Quality Assessment in California

Jucheol Moon<sup>1</sup> , Jin Gi Hong<sup>2</sup> and Tae-Won Park<sup>3,\*</sup> 

<sup>1</sup> Department of Computer Engineering and Computer Science, California State University, Long Beach, CA 90840, USA; jucheol.moon@csulb.edu

<sup>2</sup> Department of Civil Engineering and Construction Engineering Management, California State University, Long Beach, CA 90840, USA; jingi.hong@csulb.edu

<sup>3</sup> Department of Earth Science Education, Chonnam National University, Gwangju 61186, Korea

\* Correspondence: park2760@jnu.ac.kr

**Abstract:** Motor vehicle traffic is recognized as one of the critical factors that causes air pollution; however, the relationship between traffic volume and air pollutant concentrations is unclear, especially at a local level. Traditional traffic volume monitoring systems collect traffic data through counting the number of vehicles, using either sensors or surveillance cameras, but they have clear limitations such as they can only monitor certain areas and specific occasions. To overcome such limitations, we introduce a method of monitoring traffic volume in the local area by collecting estimated travel times for virtual trips in Google Maps. We began collecting the data in January 2020; ironically, the COVID-19 pandemic provided a natural experimental environment of showing unusual trends in traffic volume and unexpected changes in air pollutants. We demonstrate monthly traffic volumes in urban areas and analyze the correlation of traffic volume with typical traffic-related air pollutants using the proposed traffic volume monitoring method.

**Keywords:** traffic volume; air pollutant; big data; COVID-19



**Citation:** Moon, J.; Hong, J.G.; Park, T.-W. A Novel Method for Traffic Estimation and Air Quality Assessment in California. *Sustainability* **2022**, *14*, 9169. <https://doi.org/10.3390/su14159169>

Academic Editor: Joana Ferreira

Received: 23 June 2022

Accepted: 22 July 2022

Published: 26 July 2022

**Publisher's Note:** MDPI stays neutral with regard to jurisdictional claims in published maps and institutional affiliations.



**Copyright:** © 2022 by the authors. Licensee MDPI, Basel, Switzerland. This article is an open access article distributed under the terms and conditions of the Creative Commons Attribution (CC BY) license (<https://creativecommons.org/licenses/by/4.0/>).

## 1. Introduction

The volume and flow of traffic is considered as direct or indirect determinants of the level of air quality especially in urban areas or any locations near heavily traveled roads. The exposure to traffic-related emissions has led to concerns of potential adverse health effects for many years [1]. Motor vehicle traffic is seen as a leading cause of air quality contamination in many urban areas [2–4]. In particular, the traffic-related particulate pollution (e.g., PM<sub>2.5</sub>) is reported to contribute up to 90% of air pollution in some cities in developing countries [5,6]. In the United States and many European countries, the transport sector is also considered the largest emitter, particularly of nitrogen oxides (NO<sub>x</sub>) and carbon monoxide (CO) [7,8]. The link of traffic flows to air pollutant concentrations exists up to a certain extent; however, their intertwined relationship still remains relatively unknown and perplexing by temporal variation and specific locality. Understanding traffic patterns, related emissions, and impacts at local (state) and national scales is critical for decisive policy options and regulations and traffic assignment studies [9]. The complexity of traffic flows and emissions may also involve other related factors such as congestion, vehicle type, land development, local economy, and population. This raises the importance of traffic data measurement methods and how accurately it interprets the air quality assessment.

Traffic data is traditionally collected by conducting traffic volume (vehicle) counting at random points on high-volume roads (e.g., highway corridors). A common source of such traffic data is usually monitored from remote traffic sensors (loop detector) and/or streaming videos captured from surveillance cameras [6,10–12]. Some recent studies used the traffic applications provided by Google Maps, where traffic intensity is simply identified by several representative colors (e.g., green-fast moving or red-congestion) [13,14] Local

(or minor) road counting is uncommon despite their extensive mileage and considerable daily vehicle-miles traveled (DVMT) commuting flows. Local road traffic data are typically collected only for specific occasions such as road development or project improvement, thus limiting provision of timeliness estimates of complete travel and traffic information with breadth of data collection coverage. It is important to assess the broad geographical coverage of measurements at continuous counting sites because traffic activity varies spatially not only by type of roads but also by regions (e.g., urban and rural areas) [15]. In addition, traffic volume is also sensitive to temporal variations: high diurnal traffic patterns during weekday commuting hours and low traffic on the weekends. However, the regular and well-known patterns of traffic may also be affected by other unforeseen factors and events, which in this case, the traffic flow and travel time are hardly predictable and quantifiable. Although traffic measurements are comparatively rare on such occasions, they may provide meaningful analysis to characterize traffic behavior in conjunction with air emissions.

The surge of the unprecedented COVID-19 pandemic has significantly affected the patterns of human activity, traffic, and air quality, especially in 2020 and 2021. Many countries around the world have restricted usual daily routines and restrained domestic and international travel simply to minimize the spread of the virus. As a result, there has been a reasonably unusual trend of vehicular traffic operations and also changes in air quality levels reported in various recent studies [16–22]. It is clear that the implementation of such restrictions changes commuting flows and leads to prominent changes in air pollution levels. The state of California issued a statewide executive order for all individuals to stay home on March 19, 2020 (Executive Order N-33-20) [23]. This order meant that most Californians had to work from home which altered the usual sight of the heavily traveled roads in California. The transportation sector is the largest contributor of greenhouse gas (GHG) emissions in California: the mobile source emissions contributed up to 90% of (NO<sub>x</sub>), 90% of diesel particulate matter and 50% of CO<sub>2</sub>e GHG emissions [24].

The state government's stay-at-home order in 2020 gave us an opportunity to investigate the comparative traffic volume analyses. In this study, we propose a novel method of monitoring traffic volume using a "big data" approach to overcome the limits of the traditional methods. We explore the monthly time-series traffic distribution of California for the entire years of 2020 and 2021, primarily focusing on January, February, and March using the proposed method. These months are taken into further consideration as the stay-at-home order became effective in March, 2020, and focusing on these three months of consecutive years allows a fair comparative analysis with no seasonal variation. Furthermore, we examine the correlation of traffic data with two typical traffic-related air pollutants, NO<sub>2</sub> and CO, respectively. To date, there have been no similar studies conducting quantitative traffic data collection and analysis and its degree of relationship with the air pollutant concentrations during the pandemic over the past 2 years reported for the state of California.

## 2. Data

In this section, we explain how we collected traffic data from Google Maps and air pollutant data from an Air Quality System database.

### 2.1. Traffic Data

The traffic data were collected from Google Maps using an implemented simulation software. The software was designed to collect the estimated travel time and the travel distance for a given pair of a starting zip code and a destination zip code at the time of executing it from Google Maps. Particularly, the geographic centers of the pair of the zip codes serve as the starting point and the destination. To generate realistic pairs of starting zip codes and destination zip codes, the pairs of zip codes of morning commuters with self-driving were selected from the 2012 California Household Travel Survey (CHTS), which is a statewide survey conducted every 10 years. We obtained 11,238 unique pairs of zip codes of the home and work addresses of morning commuters in the survey. For each pair

of zip codes, we query a virtual travel once every 90 min between 5:00 a.m. to 11:00 a.m. during weekdays except holidays, and the time of the query is arbitrarily selected within a 90 min time window at every time. The data collection began on 6 January 2020, and the total number of the queried virtual travels is 23.4 million until the end of 2021.

### 2.2. Air Pollutant Data

The data on air quality and chemicals in the air are obtained from the Air Quality System (AQS) database, which is reported to the United States Environmental Protection Agency (EPA). This data is collected from a number of sensors positioned throughout the United States, Puerto Rico, and the U.S. Virgin Islands. The data is collected continuously and reported to the EPA as hourly averages over a sample duration of 1 h each, and we select data collected at sensors located only in California. Figure 1 shows the names and locations of EPA sites. The sites measure the level of a large amount of different chemical compounds present in the air. In this study, we use NO<sub>2</sub> and CO chemicals.

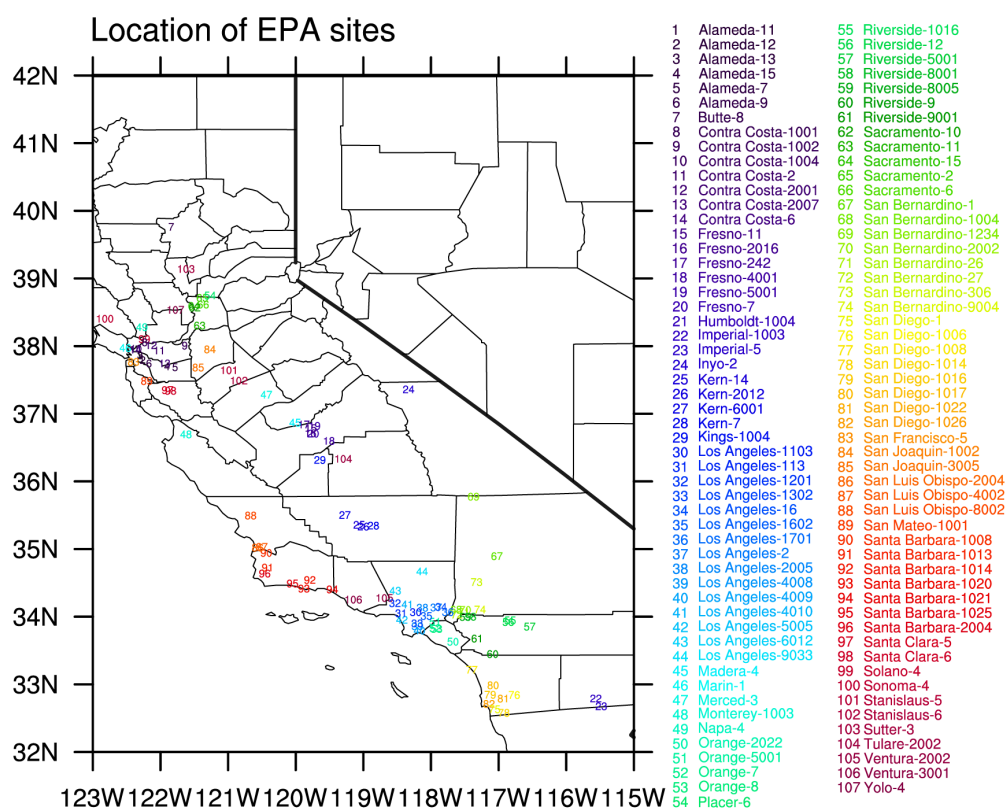


Figure 1. Names and locations of EPA sites used in this study.

The chemical data in the AQS database is made accessible through the AirData website. This site offers several ways to view the chemical data. We made use of the AQS Application Programming Interface (API) to access the data. The API allows us to write custom queries to access data from only the relevant sites, chemicals, dates, and times. We implemented software to build and execute the API requests on the AQS database. Each data point contains the date and time of the chemical measurement, a unique site identifier, the precise location of the site, and the measurement of a given chemical.

### 3. Methodology

In this section, we propose a novel method of how the amount of traffic near an EPA site is estimated using the collected traffic data and explain the data analysis method.

#### 3.1. Traffic Variables

The *travel time per mile* at time  $t$  from an origin  $zip$  to a destination  $zip'$  ( $f_{t,zip \rightarrow zip'}$ ) is defined by

$$f_{t,zip \rightarrow zip'} = \frac{e_{t,zip \rightarrow zip'}}{d_{t,zip \rightarrow zip'}} \quad (\text{minutes/mile}) \quad (1)$$

where  $e_{t,zip \rightarrow zip'}$  represents the travel time at time  $t$  from  $zip$  to  $zip'$  in minutes and  $d_{t,zip \rightarrow zip'}$  is the travel distance at time  $t$  from  $zip$  to  $zip'$  in miles. Figure 2 shows an example of calculating travel time per mile.

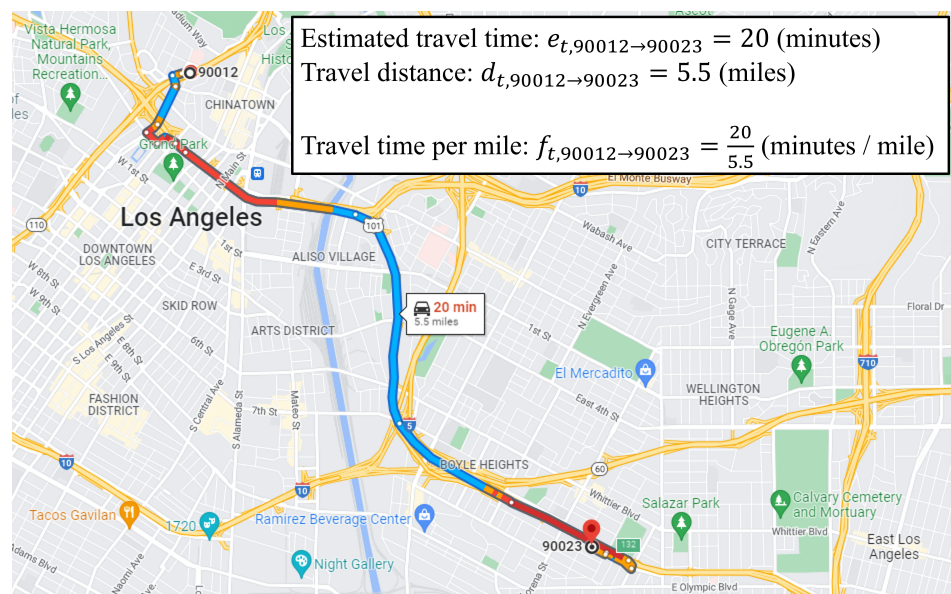


**Figure 2.** An example of calculating the travel time per mile at time  $t = 2022-04-19$  15:00:00 from the origin zip code 90012 to the destination zip code 90023. The map was captured from [maps.google.com](https://maps.google.com), accessed on 19 April 2022.

The *average out-travel time per mile* at time  $t$  from an origin  $zip$  ( $g_{t,zip}$ ) is defined by

$$g_{t,zip} = \frac{1}{|Z|} \sum_{zip' \in Z} f_{t,zip \rightarrow zip'} \quad (\text{minutes/mile}) \quad (2)$$

where  $Z$  is a set of destination zip codes in the collected traffic data. Figure 3 shows an example of calculating the average out-travel time per mile.

The *region of an EPA site* ( $R_{epa}$ ) is defined by a circular area within a radius ( $r$ ) centered by the latitude ( $x_{epa}$ ) and the longitude ( $y_{epa}$ ) of the EPA site.

$$R_{epa} = \{(x, y) | (x - x_{epa})^2 + (y - y_{epa})^2 \leq r^2\} \quad (3)$$

where  $(x, y)$  is a pair of latitude and longitude. In this study, we set the radius  $r = 10$  km.

The *region of a zip code* ( $R_{zip}$ ) is defined by an area within the boundary of the zip code.

$$R_{zip} = \{(x, y) | (x, y) \text{ within the boundary of the zip code}\} \quad (4)$$

where  $(x, y)$  is a pair of latitude and longitude. Figure 4 shows an example of  $R_{epa}$  and  $R_{zip}$ .

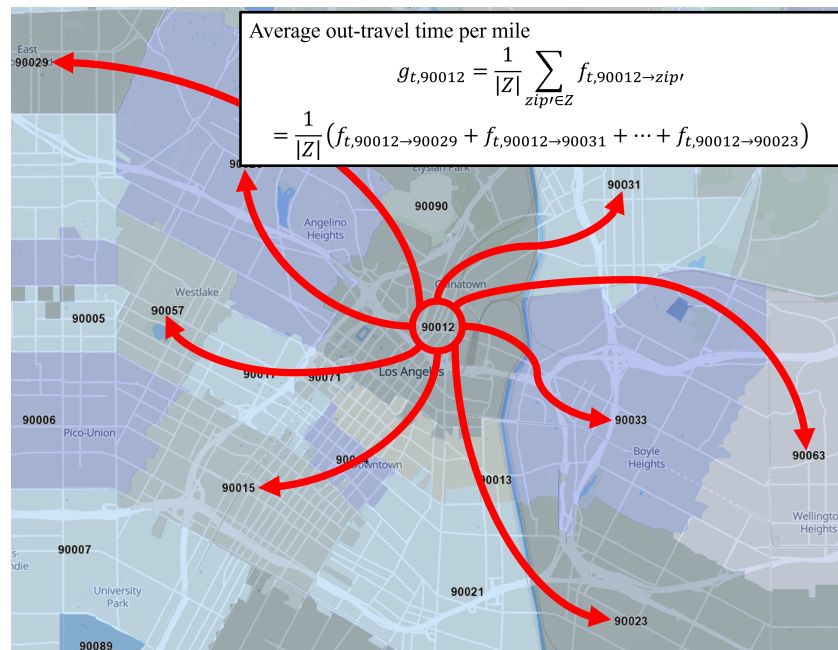


**Figure 3.** An example of calculating average out-travel time per mile at time  $t$  from the zip code 90012. The map is captured from [www.unitedstateszipcodes.org/ca/](http://www.unitedstateszipcodes.org/ca/), accessed on 19 April 2022.

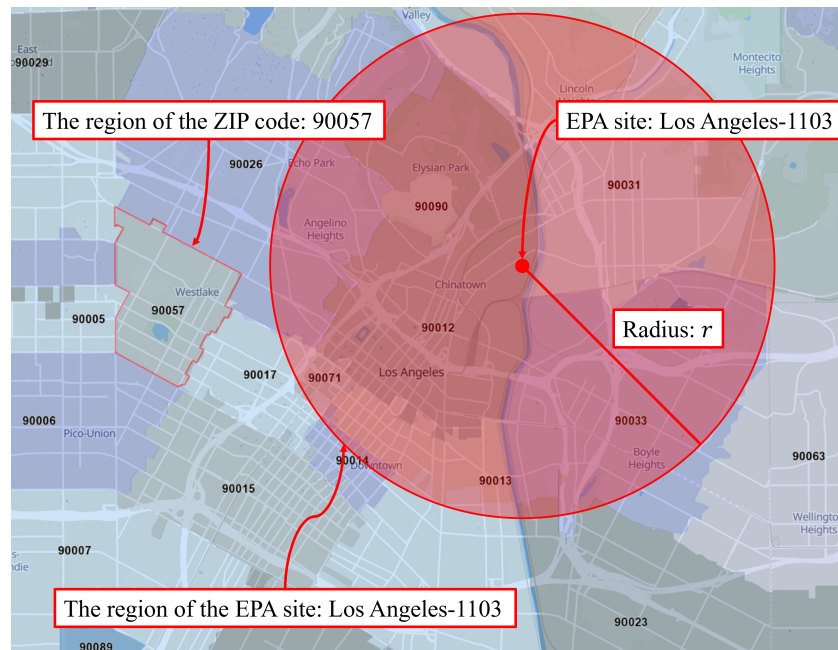


**Figure 4.** An example of the region of an EPA site and zip codes. The map was captured from [www.unitedstateszipcodes.org/ca/](http://www.unitedstateszipcodes.org/ca/), accessed on 19 April 2022.

The *weight factor* between the region of a zip code and the region of an EPA site ( $w_{epa,zip}$ ) is defined by

$$w_{zip,epa} = \frac{|R_{zip} \cap R_{epa}|}{|R_{zip}|} \tag{5}$$

where  $|R|$  represents the area of  $R$ . The weight factor can be interpreted as a ratio of the intersection area between  $R_{epa}$  and  $R_{zip}$  compared to  $R_{zip}$ .

The *traffic volume* of an EPA site at time  $t$  ( $q_{t,epa}$ ) is defined by

$$q_{t,epa} = \sum_{zip \in \{zip | w_{zip,epa} > 0\}} w_{zip,epa} \cdot g_{t,zip} \text{ (minutes/mile)} \quad (6)$$

The traffic volume of an EPA site is the weighted sum of average out-travel time per mile at time  $t$  from regions of zip codes which are overlapped with the region of the EPA site.

The traffic data is collected at a given time by the implemented software; therefore, we view the traffic volume  $q$  as a snapshot at time  $t$ . Here, times are moments; hence, they are discrete values in this study.

The *average traffic volume* of an EPA site from time  $t_1$  to time  $t_2$  ( $Q_{t_1,t_2,epa}$ ) is defined by

$$Q_{t_1,t_2,epa} = \frac{1}{|T|} \sum_{t \in T} q_{t,epa} \text{ (minutes/mile)} \quad (7)$$

where  $T = \{t | t_1 \leq t < t_2\}$ .

### 3.2. Data Analysis

We will show the following using the proposed traffic volume of the EPA site:

- Average traffic volume of each EPA site;
- Time series of the average traffic volumes of EPA sites in metropolitan areas;
- Differences in the average traffic volume, NO<sub>2</sub>, and CO between 2020 and 2021;
- Correlation between the traffic volume and NO<sub>2</sub>/CO.

We began collecting traffic data on 6 January 2020. After the first case of COVID-19 in California was confirmed by Center for Disease Control and Prevention (CDC) on 26 January 2020, the number of positive test cases increased in a short amount of time [25]. On 19 March 2020, California's governor issued a stay-at-home order, in which people were encouraged to stay at home and avoid going out [23]. Considering a timeline of California in the COVID-19 pandemic, we define the three-time periods:

- First period: 6 January 2020 to 19 March 2020 ;
- Second period: 6 January 2021 to 19 March 2021;
- All periods: 6 January 2020 to 31 December 2021.

## 4. Results

In this section, we present the use of the proposed method to calculate the traffic volume of EPA sites.

### 4.1. Traffic Volume

Before we show the results of our comparative study of two periods, we present the overall traffic volumes of EPA sites from 6 January 2020 to 31 December 2021. Figure 5 shows the average traffic volume of each EPA site for all periods. The colored circles show the regions of EPA sites ( $R_{epa}$ ), and the color of each circle represents the average traffic volume of the EPA site. We can see that the traffic volumes of EPA sites located in metropolitan areas such as San Francisco or Los Angeles are remarkably higher than the ones of EPA sites located in rural areas. The red and blue boxes in Figure 5 show the approximated boundaries of the San Francisco Area (SFA) and the Los Angeles Area (LAA), respectively. The next higher traffic volumes are found in the Sacramento, San Diego, and Fresno areas, and this is well-matched with real traffic congestion [26]. In addition, we observed that the overall distribution of traffic volumes is similar to the distribution of motor vehicle accidents [27]. (Please refer to Figure 1 in [27].) Generally, our proposed method represents the real-world traffic phenomenon accurately.

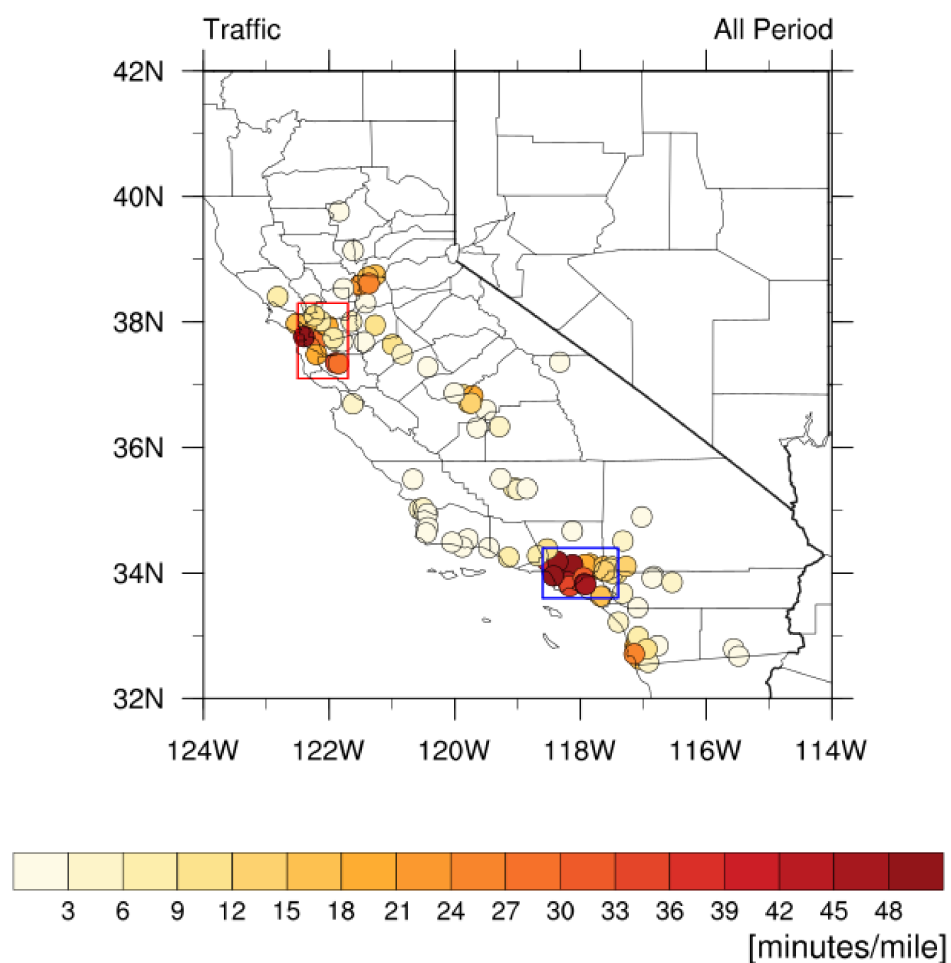


**Figure 5.** Spatial distribution of the average traffic of each EPA site from January 2020 to December 2021 (unit: minutes/mile). The circles show the regions of EPA sites, and the color (light yellow to dark red) of each circle represents the average traffic volume of the EPA site. Red and blue boxes indicate the boundaries of the San Francisco Area and the Los Angeles Area, respectively.

Due to the stay-at-home order and its prominent effect in urban areas, we expect that the amount of traffic is reduced. To verify this premise, we show time series of the monthly traffic volumes of EPA sites in the SFA and the LAA during all periods. The traffic volumes of the SF area and the LA area are the values averaged for the 18 and 24 sites that belong to the SF area and the LA area, respectively. The traffic volumes in both areas drastically reduced after the stay-at-home order, and they gradually increased until the end of 2021 as shown in Figure 6. We also can see that the monthly traffic volumes of the are higher than the traffic volumes of the SFA for every month. The traffic congestion in the LAA is commonly known as worse than the traffic congestion in the SFA [26], as shown in Figure 6.

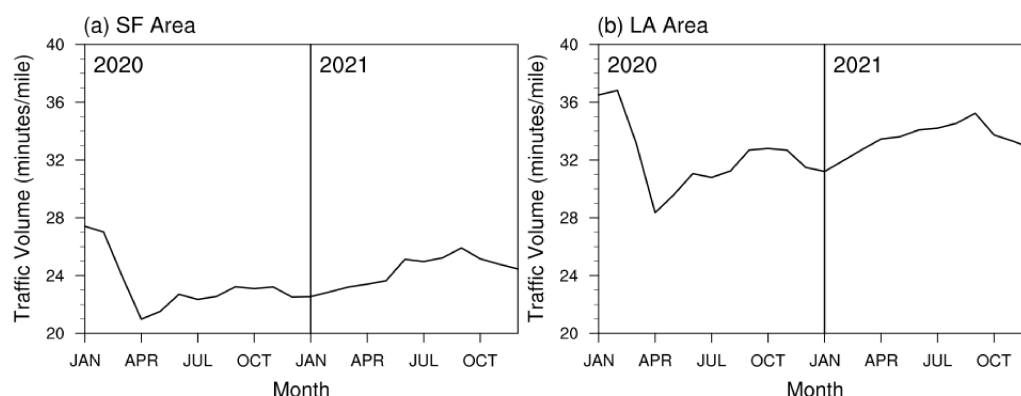


**Figure 6.** Monthly time series of traffic volume (unit: minutes/mile) in (a) the San Francisco Area and (b) the Los Angeles Area.

#### 4.2. Traffic Volume and Air Pollution

We analyzed the changes in traffic volumes in January, February, and March in 2021 and compared them to those in 2020 for interpreting the quantitative variations of traffic volume before and after the stay-at-home order. Furthermore, we quantified the changes in air quality ( $\text{NO}_2$  and CO concentrations) in 2020 and 2021. The traffic volumes,  $\text{NO}_2$ , and CO concentrations in 2020 and 2021 are the values averaged for each year. The comparative analysis is mainly focused on the same months in 2020 and 2021, because  $\text{NO}_2$  and CO concentrations are strongly dependent upon seasonal variation [28]. Figure 7 shows a contrasting distinction of traffic volume,  $\text{NO}_2$ , and CO concentrations in percentage by subtracting 2020 from 2021. Both the SFA and the LAA showed 10~20% traffic reduction in January and February, which is supported by the results on traffic change before and after the state's order estimated on highways [27]. In addition, the SFA with relatively lower traffic volume showed more significant decreases in traffic volume due to the order (Figure 7). A decrease in the concentration of  $\text{NO}_2$  and CO in the atmosphere can be attributed to the significant reduction in vehicular emission after the order. Because the state's order was issued on 19 March 2020, the traffic volume in March 2020 was already low (Figure 6), and there was no significant difference in traffic volume in March 2021. In this regard, the concentration of  $\text{NO}_2$  and CO in March also did not change significantly. Therefore, the SFA with greater traffic volume reduction also resulted in a greater decrease in  $\text{NO}_2$  and CO concentrations in 2021 compared to those in 2020. Based on this perspective, a previous study also inferred the traffic reductions associated with COVID-19 from a decrease in  $\text{NO}_x$ ,  $\text{PM}_{2.5}$ , and  $\text{O}_3$  in Southern California [17].

Many previous studies had no choice but to indirectly estimate the traffic volume near the air quality observation sites, and the traffic volume could be calculated around the specific roads such as highways. However, the new method introduced in this study can be used to calculate traffic volume in close proximity to the EPA sites. Therefore, it is possible to analyze the direct comparison between traffic volume and air pollutants at each site. Figure 8 shows correlation coefficients between  $\text{NO}_2$  and CO concentrations and traffic volume for the first, second, and all periods. Sites around big cities with higher traffic volume (e.g., the SFA, the LAA, Fresno, and San Diego) show higher correlation coefficient values. This indicates that variations of  $\text{NO}_2$  and CO concentrations are more directly related with traffic changes under the condition of heavy traffic. On the other hand,  $\text{NO}_2$  and CO concentrations in rural areas with low traffic volume are not sensitive to changes in traffic volume but are controlled by other factors such as weather. This relationship based on the threshold of traffic volume can be observed accurately in comparison before and after the stay-at-home order. In comparison to the correlation of all periods (Figure 8a,b),  $\text{NO}_2$  and CO concentrations near large cities in the first period (i.e., before the order) are more strongly correlated to traffic changes (Figure 8c,d). In the second period when traffic volumes were decreased due to the order, only a few areas showed a positive



correlation coefficient, but many other areas appeared to be either negatively correlated or uncorrelated (Figure 8e,f). Therefore, the air quality was not controlled by traffic volume itself but possibly by other sources (e.g., factory, home, and wildfire) and subsequent environmental factors (e.g., weather) may have determined the level of air quality during the time of reduced traffic related to the COVID-19 pandemic. Because our analysis is based on daily data, traffic volumes and NO<sub>2</sub> and CO concentrations for 73 days from 6 January to 19 March 2021, were used for calculating the correlation coefficient. The 73 samples are not a small number for statistical analysis. However, since they are samples for consecutive days, it seems that they can be easily affected by a few sources. Thus, in a situation where traffic volume is limited, other factors “accidentally” affect the NO<sub>2</sub> concentration in some sites, resulting in the negative correlation.

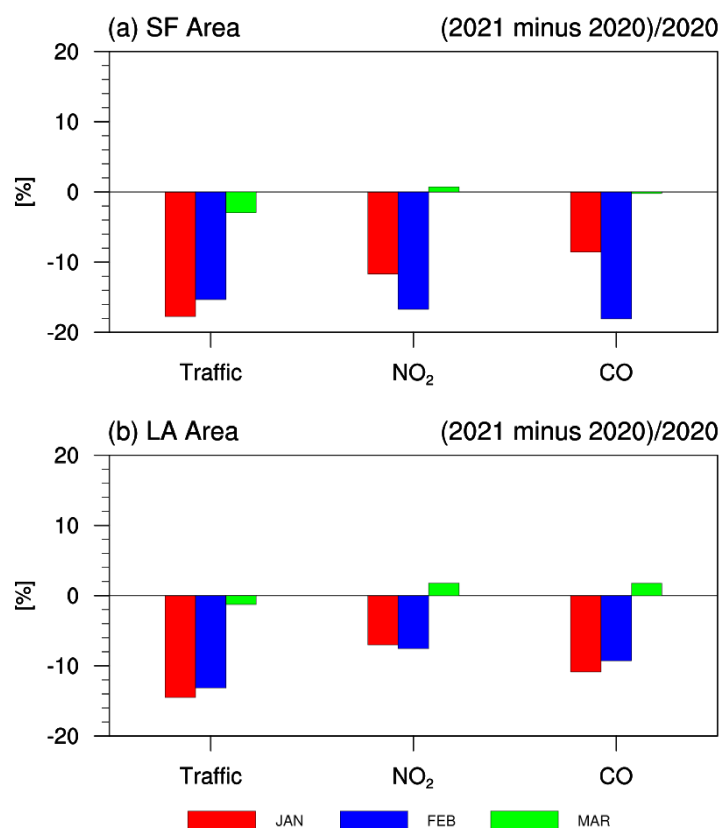


**Figure 7.** Percentage changes in traffic volume, NO<sub>2</sub>, and CO in: (a) the San Francisco Area; and (b) the Los Angeles Area in January, February, and March 2021 relative to 2020.

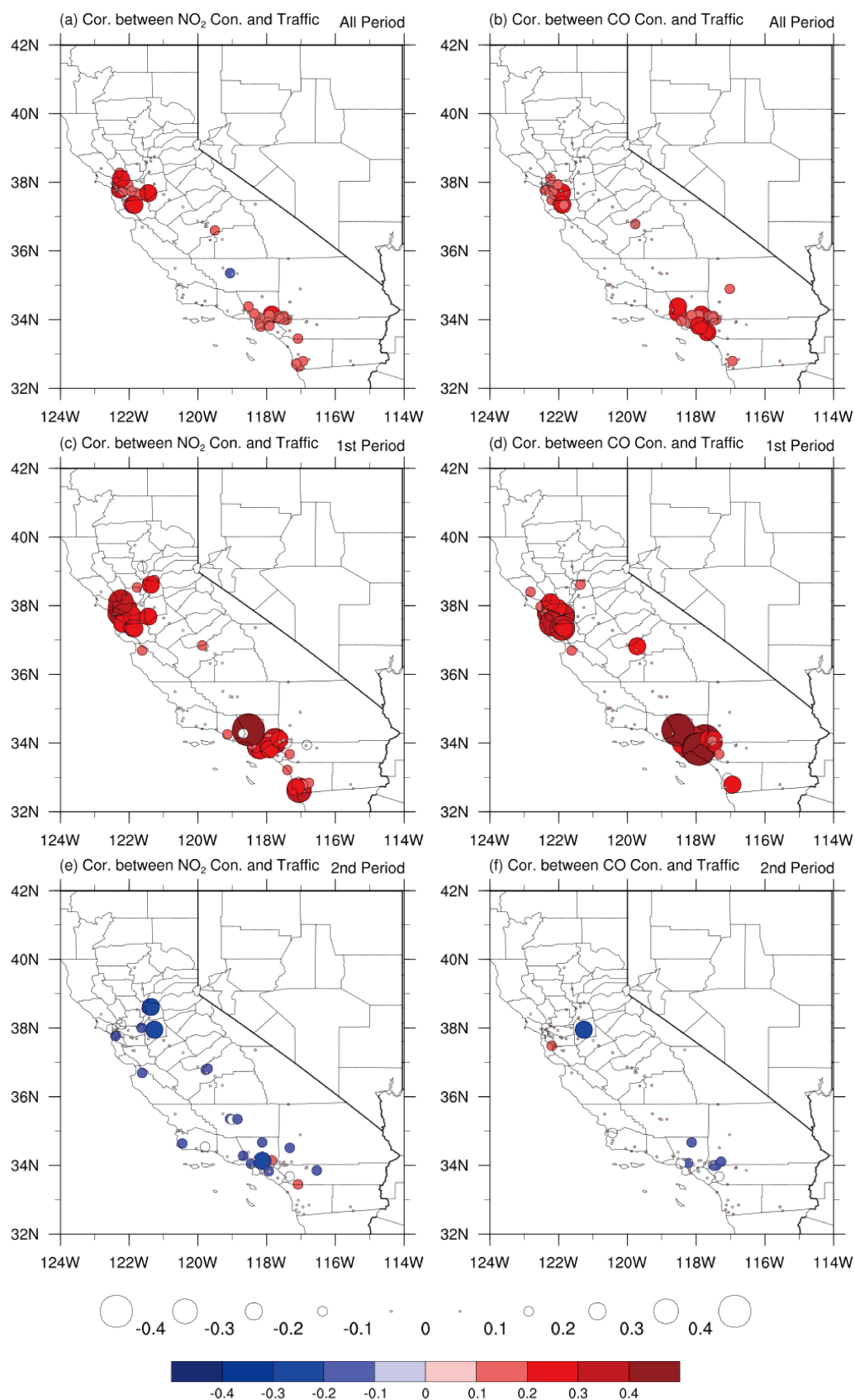


**Figure 8.** Spatial distributions of correlation coefficients for: (a,c,e) NO<sub>2</sub> concentration and traffic; and (b,d,f) CO concentration and traffic during: (a,b) all periods; (c,d) first period; and (e,f) second period. Only significant sites in the 90% confidence level are shaded.

## 5. Conclusions

This study presents a novel traffic volume monitoring method using the estimated travel times for virtual trips in Google Maps which can be applied to any region of interest. Unlike other conventional approaches of measuring traffic volume where the data collection is more centered around the particular high-volume roads, this zip-to-zip method covers and highlights all possible traffic routes near our experiment sites. A few recent studies utilized the Google Maps Traffic Application, which simply distinguishes the traffic conditions by four representative colors. This approach also contrasts to our traffic measurement using Google Maps, where the traffic volumes are derived from the time of virtual travel between zip codes.

In this study, the traffic volume was calculated using 23.4 million virtual trip queries in California from January 2020 to December 2021. We demonstrated the usefulness of the proposed method in two folds. First, we were able to check the impact of COVID-19 pandemic on traffic volume quantitatively, and second, we analyzed the correlation between traffic volume and air pollutants at each EPA site. As expected, the estimated traffic volume near the EPA sites located in the two most populated cities in California (i.e., LA and SF) markedly showed a greater volume of traffic than any other locations across the state. In addition, the influence of state-wide COVID-19-related action was evidenced in traffic volume, especially for the two cities where traffic was most prominent in the state. Furthermore, the correlation between traffic volume and two common vehicular air pollutants was found to be more significant during the first period when traffic volume was high, while the correlation during the second period is rather trivial and implies the potential interference of other determining factors such as weather or possibly industrial activities. There are some uncertainties associated with our observational approaches that could possibly be improved. As our estimation of the traffic volume near an EPA site is derived by assigning different weight averages depending on the proportion of overlapping regions of zip codes and selected perimeter of the EPA sites, it may lessen the accuracy of traffic volume estimation. If our model, considering more fragmented traffic fluxes within the region of zip code to relate with EPA site surroundings, would likely be further revamp the performance. In this study, the proposed method was utilized to estimate traffic volume around EPA sites; however, this method can be applied to broad types such as ports, airports, residential areas, or industrial complexes.

**Author Contributions:** Conceptualization, J.M., J.G.H. and T.-W.P.; methodology, J.M.; software, J.M.; validation, J.M., J.G.H. and T.-W.P.; formal analysis, T.-W.P.; investigation, J.M.; data curation, J.M.; writing—original draft preparation, J.M., J.G.H. and T.-W.P.; writing—review and editing, J.M., J.G.H. and T.-W.P.; visualization, T.-W.P.; funding acquisition, T.-W.P. All authors have read and agreed to the published version of the manuscript.

**Funding:** This study was supported by the National Research Foundation of the South Korean government (NRF-2020R1A4A3079510).

**Institutional Review Board Statement:** Not applicable.

**Informed Consent Statement:** Not applicable.

**Data Availability Statement:** Not applicable.

**Conflicts of Interest:** The authors declare no conflict of interest.

## References

1. Vette, A.; Burke, J.; Norris, G.; Landis, M.; Batterman, S.; Breen, M.; Isakov, V.; Lewis, T.; Gilmour, M.I.; Kamal, A.; et al. The near-road exposures and effects of urban air pollutants study (NEXUS): Study design and methods. *Sci. Total Environ.* **2013**, *448*, 38–47. [[CrossRef](#)] [[PubMed](#)]
2. Karagulian, F.; Belis, C.A.; Dora, C.F.C.; Prüss-Ustün, A.M.; Bonjour, S.; Adair-Rohani, H.; Amann, M. Contributions to cities' ambient particulate matter (PM): A systematic review of local source contributions at global level. *Atmos. Environ.* **2015**, *120*, 475–483. [[CrossRef](#)]

3. Khan, N.U.; Shah, M.A.; Maple, C.; Ahmed, E.; Asghar, N. Traffic flow prediction: An intelligent scheme for forecasting traffic flow using air pollution data in smart cities with bagging ensemble. *Sustainability* **2022**, *14*, 4164. [CrossRef]
4. An, S.; Ma, L.; Wang, J. Optimization of traffic detector layout based on complex network theory. *Sustainability* **2020**, *12*, 2048. [CrossRef]
5. Kinney, P.L.; Gichuru, M.G.; Volavka-Close, N.; Ngo, N.; Ndiba, P.K.; Law, A.; Gachanja, A.; Gaita, S.M.; Chillrud, S.N.; Sclar, E. Traffic impacts on PM<sub>2.5</sub> air quality in Nairobi, Kenya. *Environ. Sci. Policy* **2011**, *14*, 369–378. [CrossRef]
6. Mani, S.; Mani, F.S.; Kumar, A.; Shah, S.; Peltier, R. Traffic related PM<sub>2.5</sub> air quality: Policy options for developing Pacific Island countries. *Transp. Res. Part D Transp. Environ.* **2020**, *87*, 102519. [CrossRef]
7. The Contribution of the Transport Sector to Total Emissions of the Main Air Pollutants. Available online: [https://www.eea.europa.eu/data-and-maps/daviz/contribution-of-the-transport-sector-6#tab-chart\\_4](https://www.eea.europa.eu/data-and-maps/daviz/contribution-of-the-transport-sector-6#tab-chart_4) (accessed on 3 May 2022).
8. Batterman, S. Temporal and spatial variation in allocating annual traffic activity across an urban region and implications for air quality assessments. *Transp. Res. Part D Transp. Environ.* **2015**, *41*, 401–415. [CrossRef]
9. Zhang, Y.; Lv, J.; Ying, Q. Traffic assignment considering air quality. *Transp. Res. Part D Transp. Environ.* **2010**, *15*, 497–502. [CrossRef]
10. Wu, Y.J.; Yin, Z.; Yang, S.; Jiang, W. *Freeway Travel Time Estimation Using Existing Fixed Traffic Sensors-Phase 2*; Technical Report; University of Arizona, Department of Civil Engineering and Engineering Mechanics: Tucson, AZ, USA; Missouri University of Science and Technology, Department of Computer Science: Rolla, MO, USA, 2015.
11. Turner, S. *Defining and Measuring Traffic Data Quality*; Technical Report; Texas Transportation Institute: College Station, TX, USA, 2015.
12. Vlahogianni, E.I.; Golias, J.C.; Ziomas, I.C. Traffic flow evolution effects to nitrogen dioxides predictability in large metropolitan areas. *Transp. Res. Part D Transp. Environ.* **2011**, *16*, 273–280. [CrossRef]
13. Zalakeviciute, R.; Bastidas, M.; Buenaño, A.; Rybarczyk, Y. A traffic-based method to predict and map urban air quality. *Appl. Sci.* **2020**, *10*, 2035. [CrossRef]
14. Alexandrino, K.; Zalakeviciute, R.; Viteri, F. Seasonal variation of the criteria air pollutants concentration in an urban area of a high-altitude city. *Int. J. Environ. Sci. Technol.* **2021**, *18*, 1167–1180. [CrossRef]
15. Qu, W.; Li, J.; Yang, L.; Li, D.; Liu, S.; Zhao, Q.; Qi, Y. Short-term intersection traffic flow forecasting. *Sustainability* **2020**, *12*, 8158. [CrossRef]
16. Lee, M.; Finerman, R. COVID-19, commuting flows, and air quality. *J. Asian Econ.* **2021**, *77*, 101374. [CrossRef] [PubMed]
17. Parker, H.; Hasheminassab, S.; Crouse, J.; Roehl, C.; Wennberg, P. Impacts of traffic reductions associated with COVID-19 on southern California air quality. *Geophys. Res. Lett.* **2020**, *47*, e2020GL090164. [CrossRef] [PubMed]
18. Huang, X.; Ding, A.; Gao, J.; Zheng, B.; Zhou, D.; Qi, X.; Tang, R.; Wang, J.; Ren, C.; Nie, W.; et al. Enhanced secondary pollution offset reduction of primary emissions during COVID-19 lockdown in China. *Natl. Sci. Rev.* **2021**, *8*, nwaa137. [CrossRef] [PubMed]
19. Bauwens, M.; Compennolle, S.; Stavrou, T.; Müller, J.F.; Van Gent, J.; Eskes, H.; Levelt, P.F.; Van Der A.R.; Veefkind, J.; Vlietinck, J.; et al. Impact of coronavirus outbreak on NO<sub>2</sub> pollution assessed using TROPOMI and OMI observations. *Geophys. Res. Lett.* **2020**, *47*, e2020GL087978. [CrossRef] [PubMed]
20. Le Quére, C.; Jackson, R.B.; Jones, M.W.; Smith, A.J.; Abernethy, S.; Andrew, R.M.; De-Gol, A.J.; Willis, D.R.; Shan, Y.; Canadell, J.G.; et al. Temporary reduction in daily global CO<sub>2</sub> emissions during the COVID-19 forced confinement. *Nat. Clim. Chang.* **2020**, *10*, 647–653. [CrossRef]
21. Pan, S.; Jung, J.; Li, Z.; Hou, X.; Roy, A.; Choi, Y.; Gao, H.O. Air quality implications of COVID-19 in California. *Sustainability* **2020**, *12*, 7067. [CrossRef]
22. Heintzelman, A.; Filippelli, G.; Lulla, V. Substantial Decreases in U.S. Cities' Ground-Based NO<sub>2</sub> Concentrations during COVID-19 from Reduced Transportation. *Sustainability* **2021**, *13*, 9030. [CrossRef]
23. Governor Gavin Newsom Issues Stay at Home Order. Available online: <https://www.gov.ca.gov/2020/03/19/governor-gavin-newsom-issues-stay-at-home-order> (accessed on 20 May 2022).
24. Raju, A.S.; Wallerstein, B.R.; Johnson, K.C. Achieving NO<sub>x</sub> and Greenhouse gas emissions goals in California's Heavy-Duty transportation sector. *Transp. Res. Part D Transp. Environ.* **2021**, *97*, 102881. [CrossRef]
25. A Timeline of California in the Coronavirus Pandemic. Available online: <https://www.abc10.com/article/news/health/coronavirus/covid-19-timeline-pandemic/103-03046184-ed02-498b-b6d0-795a60646c6b> (accessed on 20 May 2022).
26. Sorensen, P. Moving Los Angeles. *ACCESS Mag.* **2009**, *1*, 16–24.
27. Shilling, F.; Waetjen, D. *Special Report: Impact of COVID19 on California Traffic Accidents*; National Academy of Sciences: Washington, DC, USA, 2020.
28. van der A, R.J.; Eskes, H.J.; Boersma, K.F.; van Noije, T.P.C.; Van Roozendaal, M.; De Smedt, I.; Peters, D.H.M.U.; Meijer, E.W. Trends, seasonal variability and dominant NO<sub>x</sub> source derived from a ten year record of NO<sub>2</sub> measured from space. *J. Geophys. Res. Atmos.* **2008**, *113*, 1–12. [CrossRef]